

# Robots of the Lost Arc: Learning to Dynamically Manipulate Fixed-Endpoint Ropes and Cables

Harry Zhang, Jeffrey Ichnowski, Daniel Seita, Jonathan Wang, and Ken Goldberg<sup>1</sup>

**Abstract**—High-speed arm motions can dynamically manipulate ropes and cables to vault over obstacles, knock objects from pedestals, and weave between obstacles. In this paper, we propose a self-supervised learning pipeline that enables a UR5 robot to perform these three tasks. The pipeline trains a deep convolutional neural network that takes as input an image of the scene with object and target. It computes a 3D apex point for the robot arm, which, together with a task-specific trajectory function, defines an arcing motion for a manipulator arm to dynamically manipulate the cable to perform a task with varying obstacle and target locations. The trajectory function computes high-speed minimum-jerk arcing motions that are constrained to remain within joint limits and to travel through the 3D apex point by repeatedly solving quadratic programs for shorter time horizons to find the shortest and fastest feasible motion. We experiment with the proposed pipeline on 5 physical cables with different thickness and mass and compare performance with two baselines in which a human chooses the apex point. Results suggest that the robot using the learned apex point can achieve success rates of 81.7% in vaulting, 65.0% in knocking, and 60.0% in weaving, while a baseline with a fixed apex across the three tasks achieves respective success rates of 51.7%, 36.7%, and 15.0%, and a baseline with human-specified task-specific apex points achieves 66.7%, 56.7%, and 15.0% success rate respectively. Code, data, and supplementary materials are available at <https://sites.google.com/berkeley.edu/dynrope/home>.

## I. INTRODUCTION

Dynamic manipulation and management of linear deformable objects such as ropes, chains, vacuum cords, charger cables, power cables, tethers, and dog leashes are common in daily life. For example, a person vacuuming may find that the vacuum’s power cord is stuck on a chair, and could use dynamic manipulation to “vault” the cord over the chair. If the first motion does not succeed, the human can try again, adapting their motion to the failure. In this paper, we explore how a robot can teach itself to perform three tasks:

**Task 1: Vaulting** The robot dynamically manipulates a cable to move from one side of an obstacle to another.

**Task 2: Knocking** The robot dynamically manipulates the cable to knock a target object off an obstacle.

**Task 3: Weaving** The robot dynamically manipulates the cable to weave it between three obstacles.

Hereafter, we use the term *cable* to refer to any 1D deformable object with minimal stiffness, such as ropes, cords, and strings. To reduce the complexity of parameterizing actions, we compute trajectories using DJ-GOMP [10], [9] that takes as input the apex point in the trajectory. This point,

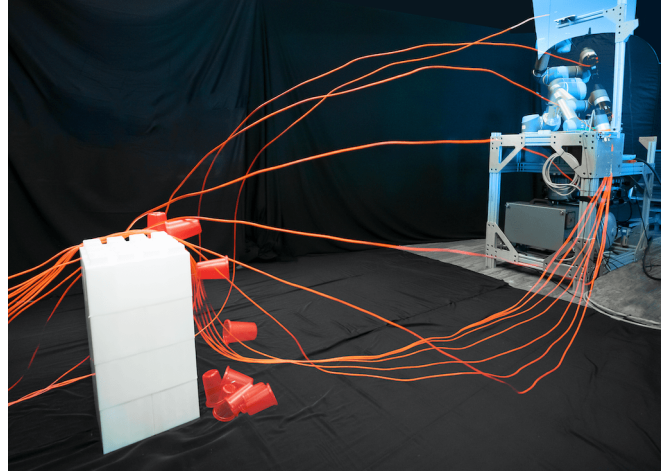


Fig. 1: Long exposure photo of a UR5 robot dynamically manipulating an orange cable fixed at one end (not shown) to knock the red target cup off the white obstacle using the learned 3d apex point and minimum-jerk robot trajectory.

combined with task-specific starting and ending arm configurations, are optimized into a single high-speed trajectory for the manipulator arm of a physical UR5 robot. We propose a self-supervised deep imitation learning pipeline that learns to predict the apex point given an image observation. Using a simulator we develop for vaulting, with a simulated UR5, we obtain an example action that completes the vaulting task. For any of the three tasks in the real world, we then have the physical UR5 continually execute actions based on the action computed in simulation, with noise added to increase dataset diversity. While the robot performs actions, one end of the cable is attached to its gripper, and the other is fixed to a wall. This process results in an autonomous procedure for collecting a large dataset. We filter the data to only include successful actions, and use the resulting data to train a deep neural network policy to predict an action (i.e., the apex point) given an image observation. Results suggest that the robot can accomplish vaulting, knocking, and weaving in a controlled environment.

This paper contributes:

- 1) Three novel dynamic cable manipulation tasks for vaulting, knocking, and weaving.
- 2) An algorithm for learning a dynamic manipulation policy for cables using a parameterized high-speed trajectory.
- 3) A simulation platform to experiment with novel tasks and policy learning.
- 4) Physical experiments evaluating the policies with a UR5 robot on 5 different cables.

<sup>1</sup>All authors are affiliated with the AUTOLab at UC Berkeley (automation.berkeley.edu). {harryzhzhang, jeffi, seita, jnwang19, goldberg}@berkeley.edu

## II. RELATED WORK

Manipulation of 1D deformable objects has applications in surgical suturing [28], [30], knot-tying [33], [8], [19], [35], untangling ropes [18], [3], [31], deforming wires [21], [22], and inserting cables into obstacles [36]; see [27] for a survey.

Various approaches have been proposed for manipulation of static cables, such as using demonstrations [29], [14], self-supervised learning [20], [24], model-free reinforcement learning [38], contrastive learning [44], dense object descriptors [32], generative modeling [34], latent space planning [16], and state estimation [43]. These prior works generally assume quasistatic dynamics to enable a series of small deformations, often parameterized with pick-and-place actions. Alternative approaches involve sliding cables [42], [46] or assuming non-quasistatic systems that enable tactile feedback [31]. This paper focuses on dynamic actions to manipulate cables from one configuration to another, traversing over obstacles and potentially knocking over objects.

More closely related to this work is that of Yamakawa et al. [39], [40], [41], [42] who focus on dynamic manipulation of cables using robot arms moving at high speeds, enabling them to model rope deformation algebraically under the assumption that the effect of gravity is negligible. They show impressive results with a single multi-fingered robot arm that ties knots by initially whipping cables upwards. Because we use fixed-endpoint cables moving at slower speeds, the forces exerted on the rope by gravity and the fixed endpoint prevent us from assuming a model where each rope joint follows the robot motion with constant time-delay, as in Yamakawa et al. Instead, we use a learning-based method and do not use specialized end-effectors. Kim and Shell [11] use a small-scale mobile robot with a cable attached as a tail to manipulate small objects by leveraging inter-object friction to drag or strike the object of interest. While their work aims to tackle dynamic cable control, it relies heavily on physics models for motion primitives that are only applicable to dragging objects via cables, and uses a RRT-based graph search algorithm to address the stochasticity in the system. We do not attempt to model cable physics, and we aim to control cables dynamically via vaulting, knocking, and weaving, and cannot rely on the same dragging motion primitives.

The proposed approach (described in Section IV) builds upon TossingBot by Zeng et al. [45], which develops a robot that can toss arbitrary objects to target bins. TossingBot uses RGBD images and employs fully convolutional neural networks [17] to get dense, per-pixel values of tossing actions, and learns a residual velocity of tossing on top of a physics model in order to jointly train a grasping and tossing policy through trial and error. We take a similar approach in dynamically manipulating by reducing the learning process to learn only the joint angles of the apex of the motion. We do not rely on any physics model of the dynamic manipulation motion, and instead, leverage a quadratic programming-based motion-planning primitive to generate a fast accelerating motion that minimizes the jerk.

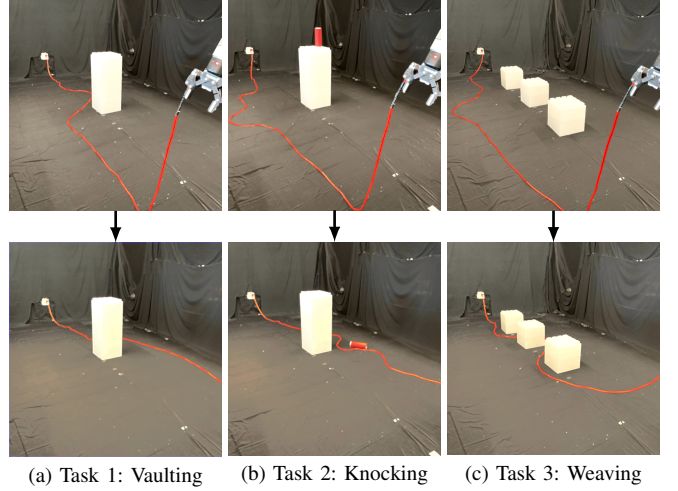


Fig. 2: Illustration of the 3 tasks: Vaulting, Knocking, and Weaving in real experiments with an orange 18-gauge cable.

## III. PROBLEM DEFINITION

Given a manipulator arm holding one end of a cable with the other end fixed (e.g., plugged into a wall), the objective is to compute and execute a high-speed arm motion that moves the cable from an initial configuration to a configuration that matches a task-dependent goal constraint.

Let  $s \in \mathcal{S}$  be the configuration of the cable and task-specific objects, including obstacles or targets. Since the configuration space  $\mathcal{S}$  is infinite-dimensional, we consider observations of the state, and focus on tasks for which the observations are sufficient to capture progress. Let  $o \in \mathcal{O}$  be the observation, and  $f_c : \mathcal{S} \rightarrow \mathcal{O}$  map a state to an observation (e.g., via a camera view). Let  $\tau_a \in \mathcal{A}$  be the action the manipulator arm takes, where  $\tau_a$  is a complete open-loop trajectory. Let  $f_S : \mathcal{S} \times \mathcal{A} \rightarrow \mathcal{S}$  be the stochastic state transition function of the cable.

Formally the objective is: for each task  $i \in \{\text{vaulting, knocking, weaving}\}$ , to learn a task-specific policy  $\pi_i : \mathcal{O} \rightarrow \mathcal{A}$ , that when given the observation  $o_0 = f_c(s_0)$  of an initial configuration  $s_0 \in \mathcal{S}$  and a goal set of observations  $\mathcal{O}_{\text{goal}} \subset \mathcal{O}$ , computes an action  $\tau_a \in \mathcal{A}$  such that  $f_c(f_S(s_0, \tau_a)) \in \mathcal{O}_{\text{goal}}$ . For each task, we define the goal set in terms of constraints, such as requiring an observation with the cable on the right side of an obstacle (Fig. 2 (a)).

The observation space needs to encode sufficient information for the policy to infer actions. For example, the observation space for vaulting should contain the location and dimensions of the obstacle to clear. We assume a camera positioned slightly above the manipulator arm, as would be common in mobile manipulator robots such as the HSR [5] and Fetch [37], and should contain sufficient information to cover the minimum observation space. Thus,  $\mathcal{O} = \mathbb{R}^{w \times h \times 3}$ , where  $w \times h$  are the dimensions of an RGB image.

Since the full set of actions  $\mathcal{A}$  is also infinite dimensional, we define a parametric trajectory function  $f_{A_i} : \mathbb{R}^3 \rightarrow \mathcal{A}$ , that, when given a point in 3D space, computes complete arm trajectory. This converts the problem to learning  $\hat{\pi}_i : \mathcal{O} \rightarrow \mathbb{R}^3$ , such that for the action  $a \in \mathbb{R}^3$  computed by the

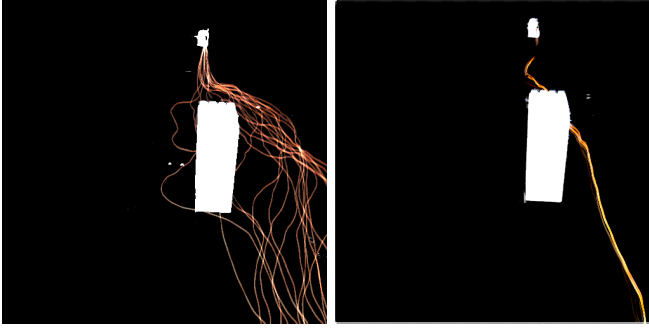


Fig. 3: **Repeatability without (left) and with (right) taut-pull reset.** Both images show the overlay of ending cable configurations after sequentially applying the same left-to-right vaulting trajectory 20 times. **Left:** without applying resets before the motion, there is high variation in ending configurations. **Right:** resetting the cable via a taut-pull before the motion results in nearly identical configurations across 20 left-to-right attempts.

---

**Algorithm 1** Iterative trainiNg for Dynamic cable manipulation (INDy)

---

**Require:** Base action of task  $i$   $a_{\beta,i}$ , a task-trajectory function  $f_{A_i}$ , a goal observation set  $\mathcal{O}_{\text{goal}}$ , number of data points  $N$ , the task's time horizon  $T$ .

- 1: Empty dataset  $\mathcal{D} = \{\}$ .
- 2: **for**  $t \in \{1 \dots N\}$  **do**
- 3:   Randomize env (obstacle size and location)
- 4:   Pull taut to reset to cable's state (updates  $s_t$ )
- 5:    $o_t \leftarrow f_c(s_t)$  {record initial observation}
- 6:   Set starting action  $a_{0:T} = a_{\beta,i}$
- 7:   **loop**
- 8:      $\tau_a \leftarrow f_{A_i}(a_{0:T})$  {compute trajectory}
- 9:     execute  $\tau_a$  on the robot (updates  $s_t$ )
- 10:    **if**  $f_c(s_t) \in \mathcal{O}_{\text{goal}}$  **then**
- 11:     **break** {success observed}
- 12:    Pull taut to reset to cable's state (updates  $s_t$ )
- 13:     $a_{0:T} \leftarrow a_{0:T} + (\text{random noise})$
- 14:     $\mathcal{D} \leftarrow \mathcal{D} \cup \{(o_t, a_{0:T})\}$
- 15: Train policy  $\pi_i(a|o)$  with  $\mathcal{D}$  to minimize Eq. 1.
- 16: **return** Trained policy for task  $i$ ,  $\pi_i(a|o)$

---

policy,  $f_c(f_S(s_0, f_{A_i}(a))) \in \mathcal{O}_{\text{goal}}$ .

## IV. METHOD

To compute fast motions that allow a robot arm to dynamically manipulate a cable, we propose a deep learning system that takes as input an image, and produces a sequence of timed joint configurations for the robot to follow. In this section, we describe the the action formulation, the training procedure, the trajectory generation algorithm, and the setup for simulated and real experiments.

### A. Hypothesis

*Repeatability:* The cable is attached to the wall, the length of the cable is fixed, and with a gentle pull, the robot can reset the cable to approximately the same starting state before each motion. The same arm trajectory will result in a similar end configuration of the cable (Fig. 3).

*Parameterized Trajectory Function:* We hypothesize that a high-speed minimum-jerk arcing manipulator-arm motion from a fixed far-left starting location, to a fixed far-right ending location, can solve many left-to-right vaulting problems by varying the midpoint location in  $(x, y, z)$  (Fig. 5 left). This reduces the problem to finding which  $\mathbb{R}^3$  input to a trajectory function  $f_{A_i}$  solves the task. This is akin to the  $\mathbb{R}^2$ -regression TossingBot [45] uses to throw object.

### B. Deep-Learning Training Algorithm

We use a self-supervised training algorithm, INDy (see Alg. 1), to learn a policy  $\pi_i$  for task  $i$ . The main inputs are: a base action for the task  $a_{\beta,i}$ , a task-trajectory function  $f_{A_i}$ , and a goal observation set  $\mathcal{O}_{\text{goal}}$ .

The training process first forms a dataset  $\mathcal{D}$  of successful observations and actions. To do this, the robot attempts the base action  $a_{\beta,i}$ . On failure, it repeatedly tries random perturbations on top of the base action until it successfully completes the task. Before each attempt, the robot self-resets the cable with a taut-pull, which makes the system repeatable (see Fig. 3). Successful observation-action pairs are added to  $\mathcal{D}$  until the data contains a user-specified number of points  $N$ . The algorithm then uses  $\mathcal{D}$  to train a convolutional neural network (CNN) [13] policy  $\pi_i$  via behavior cloning [25], [26] to output motion parameters given image observations. We parameterize the policy to produce the mean and covariance of a multivariate Gaussian, and for each data sample  $(o_t, a_{0:T}) \sim \mathcal{D}$ , optimize:

$$\mathcal{L}_{\text{MSE}} = \|\hat{a}_{0:T} - a_{0:T}\|_2^2 \quad (1)$$

where  $\hat{a}_{0:T} \sim \pi_i(a|o_t)$ , and optimization is done using the reparameterization trick [12].

### C. Min Jerk Trajectory Generation Function

The trajectory generation function  $f_{A_i} : \mathbb{R}^3 \rightarrow \mathcal{A}$  is used to reduce the output dimension of the neural network trained in Sec. IV-B, while still being able to achieve a high success rate on tasks. The exact function is a design choice, as long as it meets this criteria. We propose a function that generates motions with the following features: the arm motions are fast enough to induce a motion over the length of the cable, the apex point of the motion can be varied based on an  $\mathbb{R}^3$  input, the other points in the trajectory vary smoothly through the apex, and the motions are kinematically and dynamically feasible. In initial experiments, we observed that for the trajectory to be dynamically feasible, the trajectory generation must also limit and minimize jerk. Otherwise, acceleration changes would often be too fast for the manipulator arm to follow while burdened by the inertia of the cable.

We propose and describe a function that meets these criteria that empirically achieves high success rates in the 3 tasks. To generate a trajectory, we formulate and solve a quadratic program (QP). We first discretize a trajectory in  $H+1$  time steps, each with  $h$  seconds apart. At each time step  $t \in [0 \dots H]$ , the discretized trajectory has a configuration  $\mathbf{q}_t$ , and a configuration-space velocity  $\mathbf{v}_t$  and acceleration  $\mathbf{a}_t$ . With constraints in the QP, we enforce that the trajectory is



kinematically and dynamically feasible, starts and ends at 2 fixed arm configurations, and reaches an apex configurations defined by the output of the learned policy. The objective of the QP minimizes jerk. To make the trajectory as fast as possible, in a manner similar to GOMP [10], we repeatedly reduce  $H$  by 1 until the QP is infeasible, and use the shortest feasible trajectory. The QP takes the following form:

$$\begin{aligned} & \underset{(\mathbf{q}, \mathbf{v}, \mathbf{a})_{[0..H]}}{\operatorname{argmin}} \quad \frac{1}{2h} \sum_{i=0}^{H-1} (\mathbf{a}_{t+1} - \mathbf{a}_t)^\top Q (\mathbf{a}_{t+1} - \mathbf{a}_t) \\ & \text{s.t. } \mathbf{q}_0 \text{ is the start configuration} \\ & \quad \mathbf{q}_{\lfloor H/2 \rfloor} \text{ is the apex configuration} \\ & \quad \mathbf{q}_H \text{ is at the end configuration} \\ & \quad \mathbf{v}_0 = \mathbf{v}_H = \mathbf{0} \\ & \quad \mathbf{q}_{t+1} = \mathbf{q}_t + h\mathbf{v}_t + \frac{1}{2}h^2\mathbf{a}_t \quad \forall t \in [0..H-1] \\ & \quad \mathbf{v}_{t+1} = \mathbf{v}_t + h\mathbf{a}_t \quad \forall t \in [0..H-1] \\ & \quad \mathbf{q}_{\min} \leq \mathbf{q}_t \leq \mathbf{q}_{\max} \quad \forall t \in [1..H-1] \\ & \quad \mathbf{v}_{\min} \leq \mathbf{v}_t \leq \mathbf{v}_{\max} \quad \forall t \in [1..H-1] \\ & \quad \mathbf{a}_{\min} \leq \mathbf{a}_t \leq \mathbf{a}_{\max} \quad \forall t \in [0..H-1] \\ & \quad h\mathbf{j}_{\min} \leq \mathbf{a}_{t+1} - \mathbf{a}_t \leq h\mathbf{j}_{\max} \quad \forall t \in [0..H-1]. \end{aligned}$$

The  $Q$  matrix is a diagonal matrix that adjusts the relative weight of each joint. The QP constraints, in order, fix the start, midpoint, and end configurations ( $\mathbf{q}_0$ ,  $\mathbf{q}_{\lfloor H/2 \rfloor}$ ,  $\mathbf{q}_H$ ); fix the start and end velocity ( $\mathbf{v}_0$ ,  $\mathbf{v}_H$ ) to zero; enforce configuration and velocity dynamics between time steps ( $\mathbf{q}_{t+1}$ ,  $\mathbf{v}_{t+1}$ ); keep the joints within the specified limits of configuration ( $\mathbf{q}_{\min}$ ,  $\mathbf{q}_{\max}$ ), velocity ( $\mathbf{v}_{\min}$ ,  $\mathbf{v}_{\max}$ ), acceleration ( $\mathbf{a}_{\min}$ ,  $\mathbf{a}_{\max}$ ), and jerk ( $\mathbf{j}_{\min}$ ,  $\mathbf{j}_{\max}$ ). Unlike GOMP, we do not consider obstacle avoidance in the trajectory generation, and instead insure that there are no obstacles in the path of the arm to avoid. In practice, we fix  $h$  to be an integer multiple of the robot’s control frequency, and the initial value of  $H$  to be sufficiently large such that there is always a solution.

The input to the trajectory function constrains the midpoint configuration of the trajectory. As most trajectories lift then lower the end effector through the midpoint, the input is often the apex of the motion. With the UR5 robot, we observe that varying the first 3 joints (base, shoulder, elbow) moves the end-effector’s location in  $(x, y, z)$ . The base joint rotates left and right, while the shoulder and elbow joints lift and extend. We thus use these 3 joints to define the midpoint, while having the remaining joint configurations depend linearly on the first three. We make this function a task-specific function by constraining the start and end configurations to depend on the task. For example, we set the start configuration to be down and left, and the end configuration to be down and right, for the left-to-right vaulting task.

#### D. Simulation to Reality

We use simulation to experiment with training algorithms, and to find a feasible base action  $a_\beta$  to bootstrap the data collection process in the real world. Using simulation enables fast prototyping to efficiently assess qualitative and quantitative behavior of multiple base actions, but can suffer from a sim-to-real gap, motivating research teams to collect data

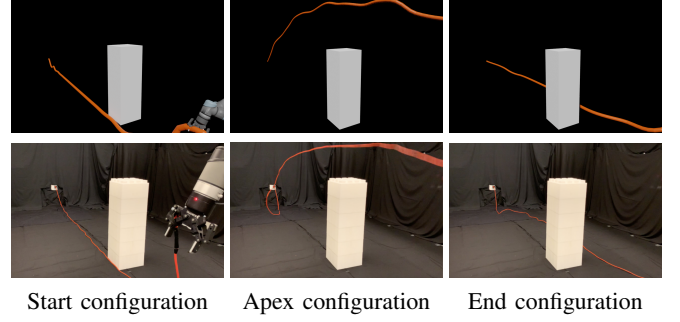


Fig. 4: Cable trajectory for data collection in **simulation (top)** vs. cable trajectory in **real (bottom)** for the vaulting task after applying the same apex point configuration.

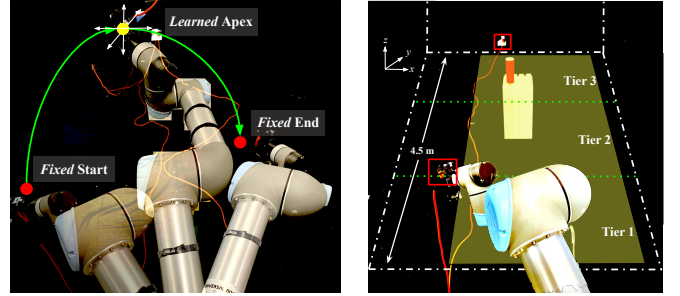


Fig. 5: **Left:** Using three points in a curve to control the trajectory of the cable. The start and end points are fixed using the arm configurations. We change the trajectory by varying the apex configuration. **Right:** Design of physical experiments. We randomize the white Lego bricks’ location within the yellow shaded area. For vaulting and knocking, the width of the yellow area is 1.5 m, and 1 m for weaving. The yellow area is broken into three difficulty tiers.

from running robots in the real world [4], [15]. Similarly, we collect data by running a physical UR5 robot, but use simulation as a means to obtain a functional action that can be improved upon when collecting data.

To model cables in simulation, we use a Featherstone [2] rigid-body simulator from BulletPhysics via Blender [1]. Cables consist of a series of small capsule links connected by spring and torsional forces. We tune the spring and torsional coefficients by decreasing bending resistance and stopping before the cable noticeably behaves like individual capsules rather than a cable, and increasing twist resistance until excessive torsion causes the capsules to separate.

When finding a feasible  $a_\beta$  to transfer to real, we only simulate vaulting. The obstacle height, radius, and location are randomized for each trial, along with the initial cable state. We use 10 different obstacle and initial cable settings in simulation, and select the input apex point with highest success rate out of 60 random points. Then, we take this apex point directly to physical experiments as the base action  $a_\beta$  to collect data, as the physical UR5 exhibits similar behavior to that in simulation after applying the predefined configurations from simulation, as seen in Fig. 4.

#### V. PHYSICAL EXPERIMENTS

We experiment with the proposed system using a physical UR5 robot grasping and dynamically manipulating a cable attached to a wall 4.5 m away, on 3 different tasks, with 5

TABLE I: Physical cables used in experiments and the number of successes in the three tasks (vaulting, knocking, weaving) using policies trained with the 18 AWG orange cable. For each cable, we evaluate with 20 trials for each task.

Type	kg	m	Vaulting	Knocking	Weaving
18 AWG orange cable	0.65	5.5	16	13	12
16 AWG white cable	0.70	5.2	16	12	12
16 AWG orange cable	0.90	6.2	4	2	2
22 AWG blue network cable	0.48	5.5	14	9	12
12 AWG blue jump rope	0.45	5.1	15	10	8

different cable types. The system obtains observations from a Logitech C270 720p webcam placed 0.75 m above the robot arm base. It scales and crops the image to a 512x512x3 segmented RGB image that feeds into a ResNet-34 [7] deep neural network implemented with PyTorch [23]. We initialize weights using He Initialization [6]. We use a UR5 arm on a fixed base because the arm can move fast enough to induce motions on the cable, and its fixed base allows us to control the experimental setup. The UR5’s joints are specified to move up to 3 rad/s, which we set as velocity constraints in the trajectory generator.

The layout of the physical experiments is shown in Fig. 5. To generate training data, we randomize the location and size of the obstacles in each trial. In the three tasks, we use large, white Lego bricks as the obstacle, which can vary in size and location. The obstacles we use for experiments are 0.15 to 0.75 m in width and 0.3 to 1.5 m in height. We test the system with 5 cables listed in Table I.

We define several *difficulty tiers* based on the distance of the obstacle to the base of the robot workstation.

**Tier 1:**  $\leq 1.5$  m | **Tier 2:** 1.5 to 3 m | **Tier 3:**  $\geq 3$  m

We evaluate Alg. 1 against two baselines:

**Baseline with Fixed Apex.** In the three tasks, for each configuration, a human annotator finds one set of apex joint angles that can accomplish the task. The apex joint angles are fixed with respect to the obstacle itself, and they remain the same across different locations of the same obstacle.

**Baseline with Varying Apex.** In vaulting and weaving, for each configuration (including obstacle size and location), a human annotator finds the apex joint angles such that the robot arm’s end effector is 15 cm above the center of mass (COM) of the obstacle, and aligned horizontally with the COM of the obstacle. For knocking, a human annotator makes the robot arm end 10 cm above the COM of the target object, and aligned horizontally with the COM.

We find the baselines from simulation, where we observe that the fixed and varying apex motions could induce enough velocity to make the cable vault the obstacle.

## VI. RESULTS

We measure the correlation between simulated and real setups, benchmark the three dynamic cable tasks, and investigate generalization to different cables. Across vaulting, knocking, and weaving, the learned apex procedure outperforms the baselines with fixed and varying apexes by 31.5% and 16.5%. Since dynamic cable manipulating is best understood via videos, we recommend the reader to check the supplementary videos on the project website.

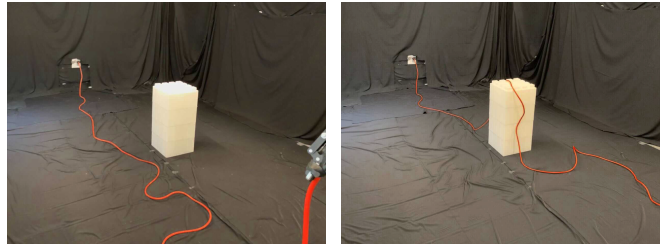


Fig. 6: **Failure mode.** The 16-gauge 6.2 m orange cable is too long for the vaulting motion. **Left:** before the motion there is too much slack. **Right:** the vaulting motion that works for shorter cables does not clear the obstacle.

TABLE II: Number of successes and failures for vaulting in simulation and physical environments across 15 trials, evaluating a different apex point on a different obstacle setting for each trial. Listed are the number of cases that succeed in both sim and real, fail in sim but succeed in real, succeed in sim but fail in real, and fail in both sim and real. The correlation between success rates in the two environments is surprisingly high.

	#Success (Simulation)	#Failure (Simulation)
#Success (Physical)	7	2
#Failure (Physical)	3	3

### A. Comparisons between Simulation and Reality

To observe correlations between cable behavior in simulation and real, we evaluate vaulting on the same set of apex point and obstacle settings in both setups. Each trial consists of a random obstacle location from all 3 difficulty tiers and a different apex point. In simulation, we use a cube mesh of the same dimension as the Lego bricks obstacle in real, and a cable of the same length and mass as the 18 AWG orange cable. Table II reports the frequency of success and failure cases across simulation and real. While the cable trajectory in simulation tends to match the trajectory of real for successes, 50% of all failed cases in real succeed in simulation under the same setting. The discrepancies between cable behavior in simulation and real are most apparent for Tier 3 scenarios, where the height achieved by the cable at the opposite end from the robot differ in the two environments. Because the cable properties cannot be perfectly tuned to match the physical properties in real, these experiments motivate the decision to transfer a base action for data collection from simulation to real, rather than a learned policy.

### B. Results for Vaulting Task

For vaulting, we collect 180 trials from manipulating the orange 5.5 m 18-gauge power extension cable, with 60 trials for each of the 3 difficulty tiers; this process took 8 hours. In each tier, we shift the obstacle vertically within the bounds of the difficulty tier and horizontally within a range of 1.5 m. We use Lego bricks to construct 6 combinations to build 6 objects of different sizes, and for each obstacle, we vary its location 10 times. Table III shows results of the trained policy on vaulting evaluated with 20 trials per tier.

### C. Results for Knocking Task

For knocking, we collect 180 trials from manipulating the orange 5.5-meter, 18-gauge power extension cable, with 60 trials for each of 3 difficulty tiers; this process took 9 hours.

TABLE III: Number of successes of the learned policy for vaulting evaluated against two baseline methods across 20 trials per difficulty tier using the 18 AWG orange cable.

Method	Tier 1	Tier 2	Tier 3
Baseline with Fixed Apex	16	13	2
Baseline with Varying Apex	19	14	7
Learned Apex	<b>20</b>	<b>18</b>	<b>11</b>

TABLE IV: Number of successes of the learned policy for knocking evaluated against two baseline methods across 20 trials per difficulty tier using the 18 AWG orange cable.

Method	Tier 1	Tier 2	Tier 3
Baseline with Fixed Apex	12	6	4
Baseline with Varying Apex	14	14	6
Learned Apex	<b>15</b>	<b>14</b>	<b>10</b>

In each difficulty tier, we use the Lego bricks as the base upon which we place the target object to be knocked, and we shift the Lego bricks base vertically within the bounds of the difficulty tier and horizontally within a range of 1.5 m. We train the policy using four different target objects: a cylinder, a tennis ball, a cup, and a rectangular box. We use Lego bricks to construct 3 combinations to build 3 bases of different sizes. For each base, we vary its locations 5 times, and for each location of the base, we vary the target on top 4 times. The result of knocking’s trained policy evaluated with 20 trials for each difficulty tier is shown in Table IV.

#### D. Results for Weaving Task

We collect 100 trials from manipulating the orange 5.5 m 18-gauge power extension cable, which took 7.5 hours. For the three obstacles, we make them identical in size. In our training data for this task, we vary the space between each object by 15 to 50 cm and we shift the obstacles horizontally within a range of 1 m. The result of weaving’s trained policy evaluated with 20 trials is shown in Table V.

#### E. Generalization to Different Cables

While the policies for the three tasks are trained using the 18-gauge orange cable, we experiment with different types of cables. The results suggest that the policy trained on the 18-gauge orange cable can transfer well to other cables of similar lengths. We observe that the same reset action can bring these cables to nearly identical starting configurations in observation space, making the policy agnostic to the cable’s type. We use the learned policy from the 18-gauge orange cable without retraining or finetuning to run the same experiments (same object sizes and locations for each task) for the three tasks with different cables and the results are shown in Table I.

TABLE V: Number of successes of the learned policy for weaving evaluated against two baseline methods across 20 trials using the 18 AWG orange cable.

Method	#Success
Baseline with Fixed Apex	3
Baseline with Varying Apex	3
Learned Apex	<b>12</b>

#### F. Limitations and Failure Cases

The learned parabolic motions are robust to object locations and shapes but have several limitations. First, the policies are learned in a highly controlled environment where the placements of the obstacles are constrained to a relatively small area. Many failure cases in vaulting and knocking are from outliers of placements that unseen during training. For example, for Tier 3 vaulting, 7 of 9 failure cases are because the horizontal shift of the obstacle exceeds the 1.5 m bound. In weaving, the horizontal shift of the obstacles is bounded into an even smaller area, so the trained weaving policy would not generalize to a variety of obstacles settings.

Second, learned policies have difficulty generalizing to cables of different lengths and masses. We conjecture that with different lengths, the amount of slack in the cables should also be different, thus decreasing the repeatability of applying the same action. With the 6.2 m cable, Tier 2 and 3 vaulting and knocking always fail in that the segment of the cable near the wall end can never be accelerated up. To show this failure mode with a longer cable, we run the policies for vaulting, knocking, and weaving trained with the 5.5 m 18-gauge cable on the 6.2 m 16-gauge cable, and we achieve 20% success rate for vaulting, 10% success rate for knocking, and 10% success rate for weaving. Figure 6 visualizes this failure case. Additionally, Table I suggests that lighter cables are likely to yield lower success rates, which may be because they often travel slower during descent, limiting the distance the cable traverses. Finally, the data generation part in Alg. 1 is inefficient since when the obstacles’ sizes and locations change, the algorithm needs to search for successful apex point again, so data generation in real is unable to record a wider variety of obstacles’ placements in an efficient manner.

## VII. CONCLUSION

We have shown that learning the apex of a parabolic motion is a promising approach for vaulting, knocking, and weaving with cables. Experimental results suggest that the proposed procedure outperforms two baseline methods in controlled environments with convex obstacles.

In future work, we will generalize the learned policy to different cable lengths and masses, and more complex obstacles and target objects. We will apply the parameterized trajectory method to other dynamic cable manipulation tasks that do not require fixed-endpoints of the cable, including bullwhipping and jump-roping. We will also explore methods to make learning more efficient.

## VIII. ACKNOWLEDGMENTS

This research was performed at the AUTOLAB at UC Berkeley in affiliation with the Berkeley AI Research (BAIR) Lab, the CITRIS “People and Robots” (CPAR) Initiative, and the Real-Time Intelligent Secure Execution (RISE) Lab. The authors were supported in part by donations from Toyota Research Institute and by equipment grants from PhotoNeo, NVidia, and Intuitive Surgical. Daniel Seita is supported by a Graduate Fellowship for STEM Diversity (GFSD). We thank our colleagues who provided helpful feedback, code, and suggestions, in particular Francesco Borrelli, Adam Lau, Huang (Raven) Huang, Priya Sundaesan, and Jennifer Grannen.

## REFERENCES

- [1] B. O. Community, *Blender – a 3D modelling and rendering package*, Blender Foundation, Stichting Blender Foundation, Amsterdam, 2018. [Online]. Available: <http://www.blender.org>
- [2] R. Featherstone, “Robot Dynamics Algorithms,” 1984.
- [3] J. Grannen, P. Sundaresan, B. Thananjeyan, J. Ichnowski, A. Balakrishna, M. Hwang, V. Viswanath, M. Laskey, J. E. Gonzalez, and K. Goldberg, “Learning Robot Policies for Untangling Dense Knots in Linear Deformable Structures,” in *Conference on Robot Learning (CoRL)*, 2020.
- [4] A. Gupta, A. Murali, D. Gandhi, and L. Pinto, “Robot Learning in Homes: Improving Generalization and Reducing Dataset Bias,” in *Neural Information Processing Systems (NeurIPS)*, 2018.
- [5] K. Hashimoto, F. Saito, T. Yamamoto, and K. Ikeda, “A Field Study of the Human Support Robot in the Home Environment,” in *IEEE Workshop on Advanced Robotics and its Social Impacts*, 2013.
- [6] K. He, X. Zhang, S. Ren, and J. Sun, “Delving deep into rectifiers: Surpassing human-level performance on imagenet classification,” in *Proceedings of the IEEE international conference on computer vision*, 2015, pp. 1026–1034.
- [7] —, “Deep Residual Learning for Image Recognition,” in *IEEE Conference on Computer Vision and Pattern Recognition (CVPR)*, 2016.
- [8] J. Hopcroft, J. Kearney, and D. Krafft, “A Case Study of Flexible Object Manipulation,” in *International Journal of Robotics Research (IJRR)*, 1991.
- [9] J. Ichnowski, Y. Avigal, V. Satish, , and K. Goldberg, “Deep Learning can Warm Start Grasp-Optimized Motion Planning,” *Science Robotics*, 2020, to appear.
- [10] J. Ichnowski, M. Danielczuk, J. Xu, V. Satish, and K. Goldberg, “GOMP: Grasp-Optimized Motion Planning for Bin Picking,” in *IEEE International Conference on Robotics and Automation (ICRA)*, 2020.
- [11] Y.-H. Kim and D. A. Shell, “Using a compliant, unactuated tail to manipulate objects,” *IEEE Robotics and Automation Letters*, vol. 2, no. 1, pp. 223–230, 2016.
- [12] D. P. Kingma and M. Welling, “Auto-Encoding Variational Bayes,” in *International Conference on Learning Representations (ICLR)*, 2014.
- [13] A. Krizhevsky, I. Sutskever, and G. E. Hinton, “ImageNet Classification with Deep Convolutional Neural Networks,” in *Neural Information Processing Systems (NeurIPS)*, 2012.
- [14] A. X. Lee, S. H. Huang, D. Hadfield-Menell, E. Tzeng, and P. Abbeel, “Unifying Scene Registration and Trajectory Optimization for Learning from Demonstrations with Application to Manipulation of Deformable Objects,” in *IEEE/RSJ International Conference on Intelligent Robots and Systems (IROS)*, 2014.
- [15] R. Lee, D. Ward, A. Cosgun, V. Dasagi, P. Corke, and J. Leitner, “Learning Arbitrary-Goal Fabric Folding with One Hour of Real Robot Experience,” in *Conference on Robot Learning (CoRL)*, 2020.
- [16] M. Lippi, P. Poklukar, M. C. Welle, A. Varava, H. Yin, A. Marino, and D. Kragic, “Latent Space Roadmap for Visual Action Planning of Deformable and Rigid Object Manipulation,” *arXiv:2003.08974*, 2020.
- [17] J. Long, E. Shelhamer, and T. Darrell, “Fully Convolutional Networks for Semantic Segmentation,” in *IEEE Conference on Computer Vision and Pattern Recognition (CVPR)*, 2015.
- [18] W. H. Lui and A. Saxena, “Tangled: Learning to Untangle Ropes with RGB-D Perception,” in *IEEE/RSJ International Conference on Intelligent Robots and Systems (IROS)*, 2013.
- [19] T. Morita, J. Takamatsu, K. Ogawara, H. Kimura, and K. Ikeuchi, “Knot Planning from Observation,” in *IEEE International Conference on Robotics and Automation (ICRA)*, 2003.
- [20] A. Nair, D. Chen, P. Agrawal, P. Isola, P. Abbeel, J. Malik, and S. Levine, “Combining Self-Supervised Learning and Imitation for Vision-Based Rope Manipulation,” in *IEEE International Conference on Robotics and Automation (ICRA)*, 2017.
- [21] H. Nakagaki, K. Kitagi, T. Ogasawara, and H. Tsukune, “Study of Insertion Task of a Flexible Wire Into a Hole by Using Visual Tracking Observed by Stereo Vision,” in *IEEE International Conference on Robotics and Automation (ICRA)*, 1996.
- [22] —, “Study of Deformation and Insertion Tasks of Flexible Wire,” in *IEEE International Conference on Robotics and Automation (ICRA)*, 1997.
- [23] A. Paszke, S. Gross, F. Massa, A. Lerer, J. Bradbury, G. Chanan, T. Killeen, Z. Lin, N. Gimelshein, L. Antiga, A. Desmaison, A. Kopf, E. Yang, Z. DeVito, M. Raison, A. Tejani, S. Chilamkurthy, B. Steiner, L. Fang, J. Bai, and S. Chintala, “PyTorch: An Imperative Style, High-Performance Deep Learning Library,” in *Neural Information Processing Systems (NeurIPS)*, 2019.
- [24] D. Pathak, P. Mahmoudieh, G. Luo, P. Agrawal, D. Chen, Y. Shentu, E. Shelhamer, J. Malik, A. A. Efros, and T. Darrell, “Zero-Shot Visual Imitation,” in *International Conference on Learning Representations (ICLR)*, 2018.
- [25] D. A. Pomerleau, “Efficient Training of Artificial Neural Networks for Autonomous Navigation,” *Neural Comput.*, vol. 3, 1991.
- [26] S. Ross, G. J. Gordon, and J. A. Bagnell, “A Reduction of Imitation Learning and Structured Prediction to No-Regret Online Learning,” in *International Conference on Artificial Intelligence and Statistics (AISTATS)*, 2011.
- [27] J. Sanchez, J.-A. Corrales, B.-C. Bouzgarrou, and Y. Mezouar, “Robotic Manipulation and Sensing of Deformable Objects in Domestic and Industrial Applications: a Survey,” in *International Journal of Robotics Research (IJRR)*, 2018.
- [28] J. Schulman, A. Gupta, S. Venkatesan, M. Tayson-Frederick, and P. Abbeel, “A Case Study of Trajectory Transfer Through Non-Rigid Registration for a Simplified Suturing Scenario,” in *IEEE/RSJ International Conference on Intelligent Robots and Systems (IROS)*, 2013.
- [29] J. Schulman, J. Ho, C. Lee, and P. Abbeel, “Learning from Demonstrations Through the Use of Non-Rigid Registration,” in *International Symposium on Robotics Research (ISRR)*, 2013.
- [30] S. Sen, A. Garg, D. V. Gealy, S. McKinley, Y. Jen, and K. Goldberg, “Automating Multi-Throw Multilateral Surgical Suturing with a Mechanical Needle Guide and Sequential Convex Optimization,” in *IEEE International Conference on Robotics and Automation (ICRA)*, 2016.
- [31] Y. She, S. Dong, S. Wang, N. Sunil, A. Rodriguez, and E. Adelson, “Cable Manipulation with a Tactile-Reactive Gripper,” in *Robotics: Science and Systems (RSS)*, 2020.
- [32] P. Sundaresan, B. Thananjeyan, A. Balakrishna, M. Laskey, K. Stone, J. E. Gonzalez, and K. Goldberg, “Learning Interpretable and Transferable Rope Manipulation Policies Using Depth Sensing and Dense Object Descriptors,” in *IEEE International Conference on Robotics and Automation (ICRA)*, 2020.
- [33] J. van den Berg, S. Miller, D. Duckworth, H. Hu, A. Wan, X.-Y. Fu, K. Goldberg, and P. Abbeel, “Superhuman Performance of Surgical Tasks by Robots Using Iterative Learning from Human-Guided Demonstrations,” in *IEEE International Conference on Robotics and Automation (ICRA)*, 2010.
- [34] A. Wang, T. Kurutach, K. Liu, P. Abbeel, and A. Tamar, “Learning Robotic Manipulation through Visual Planning and Acting,” in *Robotics: Science and Systems (RSS)*, 2019.
- [35] W. Wang and D. Balkcom, “Tying Knot Precisely,” in *IEEE International Conference on Robotics and Automation (ICRA)*, 2016.
- [36] W. Wang, D. Berenson, and D. Balkcom, “An Online Method for Tight-Tolerance Insertion Tasks for String and Rope,” in *IEEE International Conference on Robotics and Automation (ICRA)*, 2015.
- [37] M. Wise, M. Ferguson, D. King, E. Diehr, and D. Dymesich, “Fetch & Freight: Standard Platforms for Service Robot Applications,” in *IJCAI Workshop on Autonomous Mobile Service Robots*, 2016.
- [38] Y. Wu, W. Yan, T. Kurutach, L. Pinto, and P. Abbeel, “Learning to Manipulate Deformable Objects without Demonstrations,” in *Robotics: Science and Systems (RSS)*, 2020.
- [39] Y. Yamakawa, A. Namiki, and M. Ishikawa, “Motion Planning for Dynamic Knotting of a Flexible Rope With a High-Speed Robot Arm,” in *IEEE/RSJ International Conference on Intelligent Robots and Systems (IROS)*, 2010.
- [40] —, “Simple Model and Deformation Control of a Flexible Rope Using Constant, High-speed Motion of a Robot Arm,” in *IEEE International Conference on Robotics and Automation (ICRA)*, 2012.
- [41] —, “Dynamic High-Speed Knotting of a Rope by a Manipulator,” in *International Journal of Advanced Robotic Systems*, 2013.
- [42] Y. Yamakawa, A. Namiki, M. Ishikawa, and M. Shimojo, “One-Handed Knotting of a Flexible Rope With a High-Speed Multifingered Hand Having Tactile Sensors,” in *IEEE/RSJ International Conference on Intelligent Robots and Systems (IROS)*, 2007.
- [43] M. Yan, Y. Zhu, N. Jin, and J. Bohg, “Self-Supervised Learning of State Estimation for Manipulating Deformable Linear Objects,” in *IEEE Robotics and Automation Letters (RA-L)*, 2020.
- [44] W. Yan, A. Vangipuram, P. Abbeel, and L. Pinto, “Learning Predictive Representations for Deformable Objects Using Contrastive Estimation,” in *Conference on Robot Learning (CoRL)*, 2020.

- [45] A. Zeng, S. Song, J. Lee, A. Rodriguez, and T. Funkhouser, "TossingBot: Learning to Throw Arbitrary Objects with Residual Physics," in *Robotics: Science and Systems (RSS)*, 2019.
- [46] J. Zhu, B. Navarro, R. Passama, P. Fraitse, A. Crosnier, and A. Cherubini, "Robotic Manipulation Planning for Shaping Deformable Linear Objects with Environmental Contacts," in *IEEE Robotics and Automation Letters (RA-L)*, 2019.